NACA RM A50K24b

6328

NACA

RESEARCH MEMORANDUM

LIFT, DRAG, AND PITCHING MOMENT OF LOW-ASPECT-RATIO WINGS
AT SUBSONIC AND SUPERSONIC SPEEDS - TRIANGULAR
WING OF ASPECT RATIO 4 WITH NACA 0005-63
THICKNESS DISTRIBUTION, CAMBERED AND
TWISTED FOR TRAPEZOIDAL SPAN
LOAD DISTRIBUTION

By E. Ray Phelps and Willard G. Smith

Ames Aeronautical Laboratory
Moffett Field, Calif.

NATIONAL ADVISORY COMMITTEE
FOR AERONAUTICS
WASHINGTON
February 2, 1951

319.98/13

NATIONAL ADVISORY COMMITTEE FOR AERONAUTICS

RESEARCH MEMORANDUM

LIFT, DRAG, AND PITCHING MOMENT OF LOW-ASPECT-RATIO WINGS
AT SUBSONIC AND SUPERSONIC SPEEDS — TRIANGULAR
WING OF ASPECT RATIO 4 WITH NACA 0005-63
THICKNESS DISTRIBUTION, CAMBERED AND
TWISTED FOR TRAPEZOIDAL SPAN
LOAD DISTRIBUTION

By E. Ray Phelps and Willard G. Smith

SUMMARY

A wing-body combination having a triangular wing of aspect ratio 4 with NACA 0005-63 thickness distribution in streamwise planes, and cambered and twisted for a trapezoidal span load distribution has been investigated at both subsonic and supersonic Mach numbers. The lift, drag, and pitching moment of the model are presented for Mach numbers from 0.25 to 0.96 and 1.20 to 1.70 at a Reynolds number of 1.5 million. The variations of the characteristics with Reynolds number are also shown for several Mach numbers.

INTRODUCTION

A research program is in progress at the Ames Aeronautical Laboratory to ascertain experimentally at subsonic and supersonic Mach numbers the characteristics of wings of interest in the design of high-speed fighter airplanes. Variations in plan form, twist, camber, and thickness are being investigated. This report is one of a series pertaining to this program and presents results of tests of a wing-body combination having a triangular wing of aspect ratio 4 with NACA 0005-63 thickness distribution in streamwise planes and cambered and twisted for a trapezoidal span load distribution. Results of other investigations in this program are presented in references 1, 2, and 3. As in these references, the data herein are presented without analysis to expedite publication.

NOTATION

b   wing span, feet

$\bar{c}$ mean aerodynamic chord $\left(\dfrac{\int_0^{b/2} c^2\,dy}{\int_0^{b/2} c\,dy}\right)$, feet

c   projected local wing chord, feet

l length of body including portion removed to accommodate sting, inches

$\dfrac{L}{D}$ lift–drag ratio

$\left(\dfrac{L}{D}\right)_{max}$ maximum lift–drag ratio

M   Mach number

q   free–stream dynamic pressure, pounds per square foot

R   Reynolds number based on the mean aerodynamic chord

r   radius of body, inches

r_0 maximum body radius, inches

S   total projected wing area, including area formed by extending leading and trailing edges to plane of symmetry, square feet

X   distance from wing leading edge in wing reference plane, inches

x   longitudinal distance from nose of body, inches

Z   vertical distance from wing reference plane, inches

y   distance perpendicular to plane of symmetry, feet

α angle of attack of body axis, degrees

C_D drag coefficient $\left(\dfrac{drag}{qS}\right)$

C_L lift coefficient $\left(\dfrac{lift}{qS}\right)$

C_m pitching–moment coefficient referred to quarter point of mean

aerodynamic chord $\left(\dfrac{\text{pitching moment}}{qS\overline{c}} \right)$

$\dfrac{dC_L}{d\alpha}$ slope of the lift curve measured at zero lift, per degree

$\dfrac{dC_m}{dC_L}$ slope of the pitching–moment curve measured at zero lift

Subscripts

U   upper surface of wing

L   lower surface of wing

APPARATUS

Wind Tunnel and Equipment

The experimental investigation was conducted in the Ames 12–foot pressure wind tunnel and in the Ames 6– by 6–foot supersonic wind tunnel. In each wind tunnel, the Mach number can be varied continuously and the stagnation pressure can be regulated to maintain a given test Reynolds number. The air in these tunnels is dried to prevent formation of condensation shocks. Further information on these wind tunnels is presented in references 4 and 5.

The model was sting mounted in each tunnel, the diameter of the sting being about 82 percent of the diameter of the body base. The pitch plane of the model support was vertical in the 12–foot wind tunnel and horizontal in the 6– by 6–foot wind tunnel. A balance mounted on the sting support and enclosed within the body of the model was used to measure the aerodynamic forces and moments on the model. The balance was a 2–1/2–inch, four–component, strain–gage balance of the type described in reference 6.

Model

A photograph of the model mounted in the Ames 12–foot pressure wind tunnel is shown in figure 1. Plan and front views of the model and

certain model dimensions are given in figure 2. Other important geomet-
ric characteristics of the model are as follows:

Wing

    Aspect ratio 4
    Taper ratio 0
    Thickness distribution (streamwise) . . . . . . : NACA 0005–63
    Total area, S, square feet 2.007
    Mean aerodynamic chord, $\bar{c}$, feet 0.944
    Incidence, degrees . . . . : . . . . . : 0
    Distance, wing reference plane to body axis, feet . . 0

Body

    Fineness ratio (based on length l; fig. 2) 12.5
    Cross–section shape . . . . Circular
    Maximum cross-sectional area, square feet 0.1026
    Ratio of maximum cross-sectional area to wing area . 0.0509

        The twist and camber of the present wing were derived from a theo-
retical equation satisfying the linearized supersonic potential flow
equation and giving the shape of a surface for a uniform pressure distri-
bution. (See reference 7.) At the design Mach number of 1.15 and design
lift coefficient of 0.35 the span load distribution was trapezoidal,
being constant to 62.5 percent of the semispan and varying linearly from
there to zero at the tip. The section coordinates for this wing are given
in table I.

        The wing was constructed of solid steel. The body spar was also
steel and covered with aluminum to form the body contours. The surfaces
of the wing and body were polished smooth.

                        TESTS AND PROCEDURE

                        Range of Test Variables

        The characteristics of the model (as a function of·angle of attack)
were investigated for a range of Mach numbers from 0.25 to 0.96 in the
Ames 12–foot pressure wind tunnel and from 1.20 to 1.70 in the Ames
6– by 6–foot supersonic wind tunnel. The major portion of the data was
obtained at a Reynolds number of 1.5 million. Data were also obtained

for Reynolds number up to 8.0 million at a Mach number of 0.25 and up to
a Reynolds number of 3.0 million at supersonic Mach numbers.

Reduction of Data

The test data have been reduced to standard NACA coefficient form.
Factors which could affect the accuracy of these results and the correc-
tions applied are discussed in the following paragraphs.

Tunnel-wall interference.— Corrections to the subsonic results for
the induced effects of the tunnel walls resulting from lift on the model
were made according to the methods of reference 8. The numerical values
of these corrections (which were added to the uncorrected data) were, for
the results from the 12-foot wind tunnel:

$$\Delta\alpha = 0.14 \; c_L$$

$$\Delta C_D = 0.0023 \; c_L{}^2$$

No corrections were made to the pitching-moment coefficients.

The effects of constriction of the flow at subsonic speeds by the
tunnel walls were accounted for by the method of reference 9. This cor-
rection was calculated for conditions at zero angle of attack and was
applied throughout the angle-of-attack range. At a Mach number of 0.96
in the 12-foot wind tunnel, this correction amounted to a 1-percent
increase in the Mach number over that determined from a calibration of
the wind tunnel without a model in place.

For the tests at supersonic speeds, the reflection from the tunnel
walls of the Mach wave originating at the nose of the body did not cross
the model. No corrections were required, therefore, for tunnel-wall
effects.

Stream variations.— Calibration of the 12-foot wind tunnel has shown
that in the test region the stream inclination determined from tests of
a wing spanning the tunnel, with the support system at 0° angle of attack,
is less than 0.08°. The variation of static pressure is less than 0.2
percent of the dynamic pressure. No correction for the effect of these
stream variations was made.

A survey of the air stream in the 6— by 6-foot wind tunnel at super-
sonic speeds (reference 5) has shown a stream curvature only in the yaw
plane of the model. The effects of this curvature on the measured char-
acteristics of the present model are not known, but are believed to be
small as judged by the results of reference 10. The survey also

indicated that there is a static-pressure variation in the test section of sufficient magnitude to affect the drag results. A correction was added to the measured drag coefficient, therefore, to account for the longitudinal buoyancy caused by this static-pressure variation. This correction varied from as much as -0.0016 at a Mach number of 1.20 to +0.0016 at a Mach number of 1.70.

Support interference.- At subsonic speeds, the effects of support interference on the aerodynamic characteristics of the model are not known. For the present tailless model, it is believed that such effects consisted primarily of a change in the pressure at the base of the model. In an effort to correct at least partially for this support interference, the base pressure was measured and the drag data were adjusted to correspond to a base pressure equal to the static pressure of the free stream.

At supersonic speeds, the effects of support interference of a body-sting configuration similar to that of the present model are shown by reference 11 to be confined to a change in base pressure. The previously mentioned adjustment of the drag for base pressure, therefore, was applied at supersonic speeds.

Errors introduced by support system.- Clearances between moving parts in the support system in the 6- by 6-foot supersonic wind tunnel under certain conditions permitted the angle of attack to vary as much as 0.3° with no change in the angle-of-attack indicator. The clearances were discovered after inspection of the data of reference 3 showed that the drag coefficients were not the same at positive and negative lift coefficients. However, calibration of the angle-of-attack indicator during the present investigation, as well as that of reference 3, had been made in such a manner that the angles of attack and thus the lift and drag results were correct at positive lift coefficients. Further proof of this fact was obtained during the investigation of reference 3 from re-runs at several Mach numbers made in a manner to eliminate altogether the effects of the excessive clearance. The drag data from those tests (symmetrical about zero lift) agreed with those of the first series of tests at positive lift coefficient, as did the angle of attack and lift and pitching-moment coefficients.

Balance.- As the model is pitched in the vertical plane in the 12-foot wind tunnel, the weight of the model produces a change in the measured forces and moments which, for the present tests, was significant only for the chord-force measurements. The measured chord-force tare had a small discontinuity when the chord force reversed direction. Since the same discontinuity was present in the uncorrected drag data, these data were corrected for this inherent characteristic of the measuring system.

RESULTS

The results are presented in this report without analysis in order to expedite publication. Figure 3 shows the variation of lift coefficient with angle of attack and the variation of drag coefficient, pitching-moment coefficient, and lift-drag ratio with lift coefficient at a Reynolds number of 1.5 million and at Mach numbers from 0.25 to 1.70. The effect of Reynolds number on the aerodynamic characteristics at Mach numbers of 0.25, 1.20 and 1.53 is shown in figure 4. The results presented in figure 3 have been summarized in figure 5 to show some important parameters as functions of Mach number. The slope parameters in this figure have been measured at zero lift.

Ames Aeronautical Laboratory,
    National Advisory Committee for Aeronautics,
        Moffett Field, Calif.

REFERENCES

1. Smith, Donald W., and Heitmeyer, John C.: Lift, Drag, and Pitching Moment of Low-Aspect-Ratio Wings at Subsonic and Supersonic Speeds — Plane Triangular Wing of Aspect Ratio 2 With NACA 0008-63 Section. NACA RM A50K20, 1950.

2. Smith, Donald W., and Heitmeyer, John C.: Lift, Drag, and Pitching Moment of Low-Aspect-Ratio Wings at Subsonic and Supersonic Speeds — Plane Triangular Wing of Aspect Ratio 2 With NACA 0005-63 Section. NACA RM A50K21, 1950.

3. Heitmeyer, John C., and Stephenson, Jack D.: Lift, Drag, and Pitching Moment of Low-Aspect-Ratio Wings at Subsonic and Supersonic Speeds — Plane Triangular Wing of Aspect Ratio 4 With NACA 0005-63 Section. NACA RM A50K24, 1950.

4. Edwards, George G., and Stephenson, Jack D.: Tests of a Triangular Wing of Aspect Ratio 2 in the Ames 12-Foot Pressure Wind Tunnel. I — The Effect of Reynolds Number and Mach Number on the Aerodynamic Characteristics of the Wing With Flap Undeflected. NACA RM A7K05, 1947.

5. Frick, Charles W., and Olson, Robert N.: Flow Studies in the Asymmetric Adjustable Nozzle of the Ames 6- by 6-Foot Supersonic Wind Tunnel. NACA RM A9E24, 1949.

6. Olson, Robert N., and Mead, Merrill H.: Aerodynamic Study of a Wing–Fuselage Combination Employing a Wing Swept Back 63°.— Effectiveness of an Elevon as a Longitudinal Control and the Effects of Camber and Twist on the Maximum Lift–Drag Ratio at Supersonic Speeds. NACA RM A50A31a, 1950.

7. Jones, Robert T.: Estimated Lift–Drag Ratios at Supersonic Speeds. NACA TN 1350, 1947.

8. Glauert, H.: The Elements of Aerofoil and Airscrew Theory. The University Press, Cambridge, England, 1926, Ch. XIV.

9. Herriot, John G.: Blockage Corrections for Three–Dimensional–Flow Closed–Throat Wind Tunnels, With Consideration of the Effect of Compressibility. NACA RM A7B28, 1947.

10. Lessing, Henry C.: Aerodynamic Study of a Wing–Fuselage Combination Employing a Wing Swept Back 63°.— Effect of Sideslip on Aerodynamic Characteristics at a Mach Number of 1.4 With the Wing Twisted and Cambered. NACA RM A50F09, 1950.

11. Perkins, Edward W.: Experimental Investigation of the Effects of Support Interference on the Drag of Bodies of Revolution at a Mach Number of 1.5. NACA RM A8B05, 1948.

TABLE I[1]

COORDINATES FOR TWISTED AND CAMBERED TRIANGULAR WING OF ASPECT RATIO 4

Station 0 (symmetrical)		Station 2.210				Station 3.400				Station 4.250				Station 5.100			
x	z	x_U	z_U	x_L	z_L	x_U	z_U	x_L	z_L	x_U	z_U	x_L	z_L	x_U	z_U	x_L	z_L
0.000	0.000	0.000	0.127	0.000	0.127	0.000	0.196	0.000	0.196	0.000	0.244	0.000	0.244	0.000	0.293	0.000	0.293
.213	.134	.188	.270	.186	.035	.172	.330	.169	.117	.152	.373	.149	.172	.151	.416	.148	.226
.425	.185	.376	.326	.373	.002	.343	.384	.339	.087	.326	.427	.321	.146	.301	.467	.296	.205
.850	.252	.750	.390	.746	-.049	.684	.456	.678	.050	.650	.499	.644	.117	.600	.535	.593	.179
1.275	.298	1.108	.416	1.103	-.107	1.024	.498	1.018	.021	.957	.541	.950	.093	.899	.581	.891	.163
1.700	.332	1.482	.403	1.476	-.180	1.365	.521	1.357	-.011	1.281	.572	1.273	.072	1.197	.613	1.188	.149
2.550	.379	2.230	.405	2.224	-.259	2.044	.507	2.036	-.101	1.927	.595	1.918	.025	1.792	.649	1.782	.122
3.400	.406	2.961	.411	2.955	-.300	2.724	.479	2.715	-.181	2.556	.559	2.546	-.054	2.388	.653	2.377	.085
4.250	.421	3.709	.410	3.702	-.320	3.404	.451	3.395	-.221	3.201	.506	3.191	-.128	2.981	.616	2.970	.025
5.100	.425	4.440	.406	4.433	-.331	4.084	.435	4.075	-.243	3.830	.479	3.819	-.160	3.575	.543	3.564	-.052
6.800	.411	5.919	.382	5.912	-.333	5.444	.399	5.435	-.256	5.103	.429	5.093	-.187	4.764	.471	4.753	-.104
8.500	.375	7.397	.344	7.392	-.309	6.802	.354	6.794	-.243	6.378	.381	6.369	-.184	5.953	.409	5.943	-.114
10.200	.323	8.876	.293	8.871	-.269	8.162	.302	8.155	-.214	7.652	.327	7.644	-.169	7.143	.347	7.134	-.103
11.900	.260	10.355	.234	10.351	-.218	9.521	.243	9.516	-.171	8.927	.258	8.920	-.133	8.332	.286	8.325	-.077
13.600	.186	11.833	.167	11.830	-.156	10.881	.178	10.877	-.120	10.201	.193	10.196	-.085	9.520	.220	9.515	-.041
15.300	.103	13.311	.092	13.309	-.087	12.240	.105	12.238	-.059	11.475	.124	11.473	-.030	10.709	.149	10.706	.006
16.150	.057	14.058	.051	14.057	-.048	12.920	.068	12.918	-.025	12.120	.085	12.118	0	11.304	.113	11.302	.033
17.000	.009	14.789	.008	14.789	-.008	13.599	.025	13.599	-.011	12.748	.047	12.748	.033	11.898	.074	11.898	.062
Leading-edge radius: 0.046		Leading-edge radius: 0.040				Leading-edge radius: 0.037				Leading-edge radius: 0.035				Leading-edge radius: 0.032			

Station 6.800				Station 8.500				Station 10.200				Station 12.750				Station 14.875			
x_U	z_U	x_L	z_L	x_U	z_U	x_L	z_L	x_U	z_U	x_L	z_L	x_U	z_U	x_L	z_L	x_U	z_U	x_L	z_L
0.000	0.391	0.000	0.391	0.000	0.489	0.000	0.489	0.000	0.587	0.000	0.587	0.000	0.733	0.000	0.733	0.000	0.856	0.000	0.856
.131	.499	.127	.333	.104	.576	.101	.450	.086	.660	.085	.550	.047	.781	.051	.713	.025	.882	.028	.846
.259	.544	.253	.318	.224	.624	.220	.434	.171	.694	.170	.544	.096	.803	.102	.710	.050	.893	.055	.844
.515	.609	.508	.303	.430	.681	.424	.422	.342	.743	.340	.538	.215	.836	.222	.709	.102	.910	.108	.848
.772	.654	.763	.294	.652	.720	.645	.420	.512	.778	.510	.539	.314	.863	.322	.713	.153	.924	.160	.851
1.028	.688	1.018	.290	.857	.752	.849	.419	.682	.809	.680	.540	.417	.885	.426	.717	.206	.937	.214	.855
1.539	.733	1.528	.280	1.283	.800	1.274	.421	1.023	.852	1.020	.551	.637	.920	.647	.729	.311	.958	.320	.863
2.049	.758	2.037	.271	1.709	.831	1.699	.424	1.363	.885	1.360	.560	.840	.945	.851	.740	.415	.975	.425	.875
2.559	.765	2.547	.261	2.134	.850	2.124	.429	1.703	.906	1.700	.571	1.058	.965	1.070	.755	.521	.990	.531	.886
3.069	.752	3.057	.245	2.559	.855	2.549	.430	2.043	.922	2.040	.585	1.263	.982	1.275	.768	.627	1.002	.637	.896
4.087	.656	4.076	.160	3.409	.841	3.400	.430	2.724	.934	2.720	.606	1.687	1.007	1.698	.801	.838	1.022	.848	.919
5.105	.530	5.095	.082	4.259	.789	4.250	.413	3.404	.924	3.401	.624	2.113	1.019	2.123	.831	1.050	1.037	1.060	.943
6.123	.449	6.114	.061	5.106	.672	5.098	.347	4.083	.892	4.081	.633	2.538	1.022	2.547	.859	1.262	1.048	1.270	.967
7.142	.374	7.134	.063	5.953	.543	5.946	.280	4.763	.843	4.761	.636	2.964	1.019	2.971	.889	1.476	1.055	1.482	.989
8.160	.303	8.155	.081	6.801	.451	6.797	.264	5.442	.770	5.441	.624	3.390	1.009	3.395	.916	1.688	1.061	1.693	1.015
9.179	.232	9.176	.110	7.650	.370	7.647	.268	6.121	.653	6.120	.568	3.816	.992	3.819	.940	1.902	1.062	1.904	1.037
9.688	.195	9.686	.128	8.074	.328	8.072	.269	6.461	.578	6.460	.533	4.039	.982	4.040	.954	2.009	1.064	2.010	1.050
10.197	.158	10.197	.148	8.498	.292	8.498	.282	6.800	.525	6.800	.517	4.244	.969	4.244	.965	2.115	1.063	2.115	1.061
Leading-edge radius: 0.026				Leading-edge radius: 0.023				Leading-edge radius: 0.019				Leading-edge radius: 0.012				Leading-edge radius: 0.006			

[1] Locations of stations are measured in inches from plane of symmetry.

NACA

NACA RM A50K24b
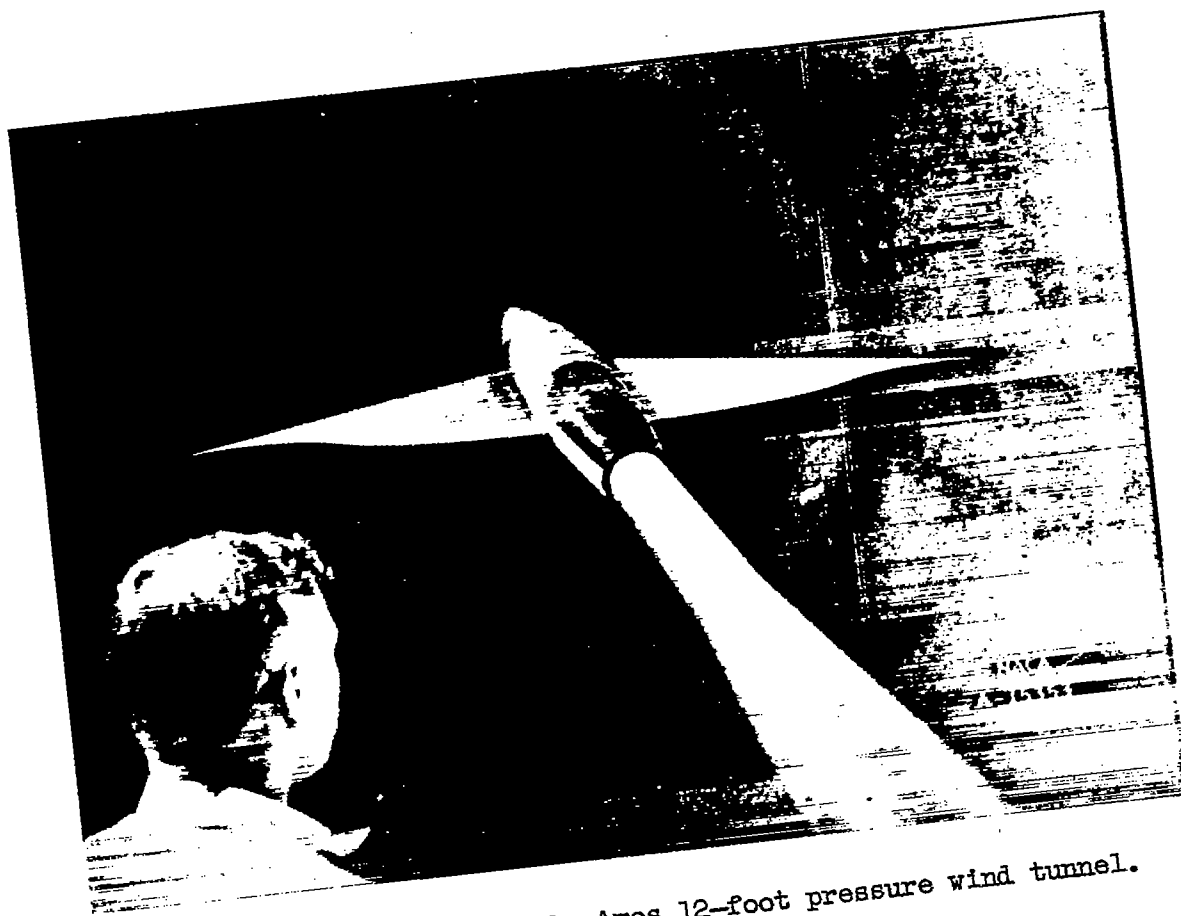
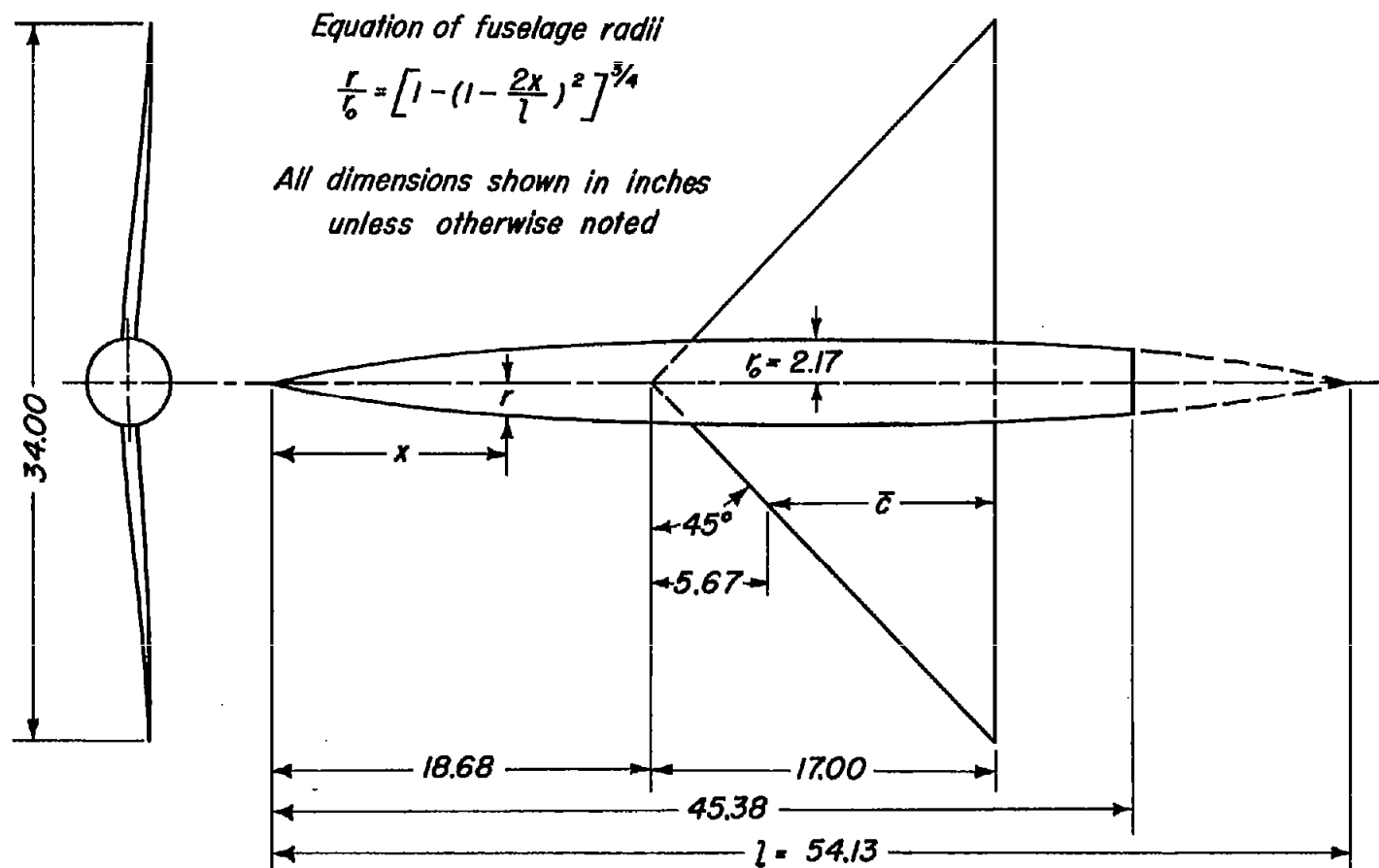Figure 1.— The model in the Ames 12—foot pressure wind tunnel.

Equation of fuselage radii

$$\frac{r}{r_o} = \left[1 - \left(1 - \frac{2x}{l} \right)^2 \right]^{3/4}$$

All dimensions shown in inches
unless otherwise noted

$r_o = 2.17$

r

x

$\bar{c}$

45°

5.67

34.00

18.68

17.00

45.38

$l = 54.13$

Figure 2.— Plan and front views of the model.

(a) C_L vs α
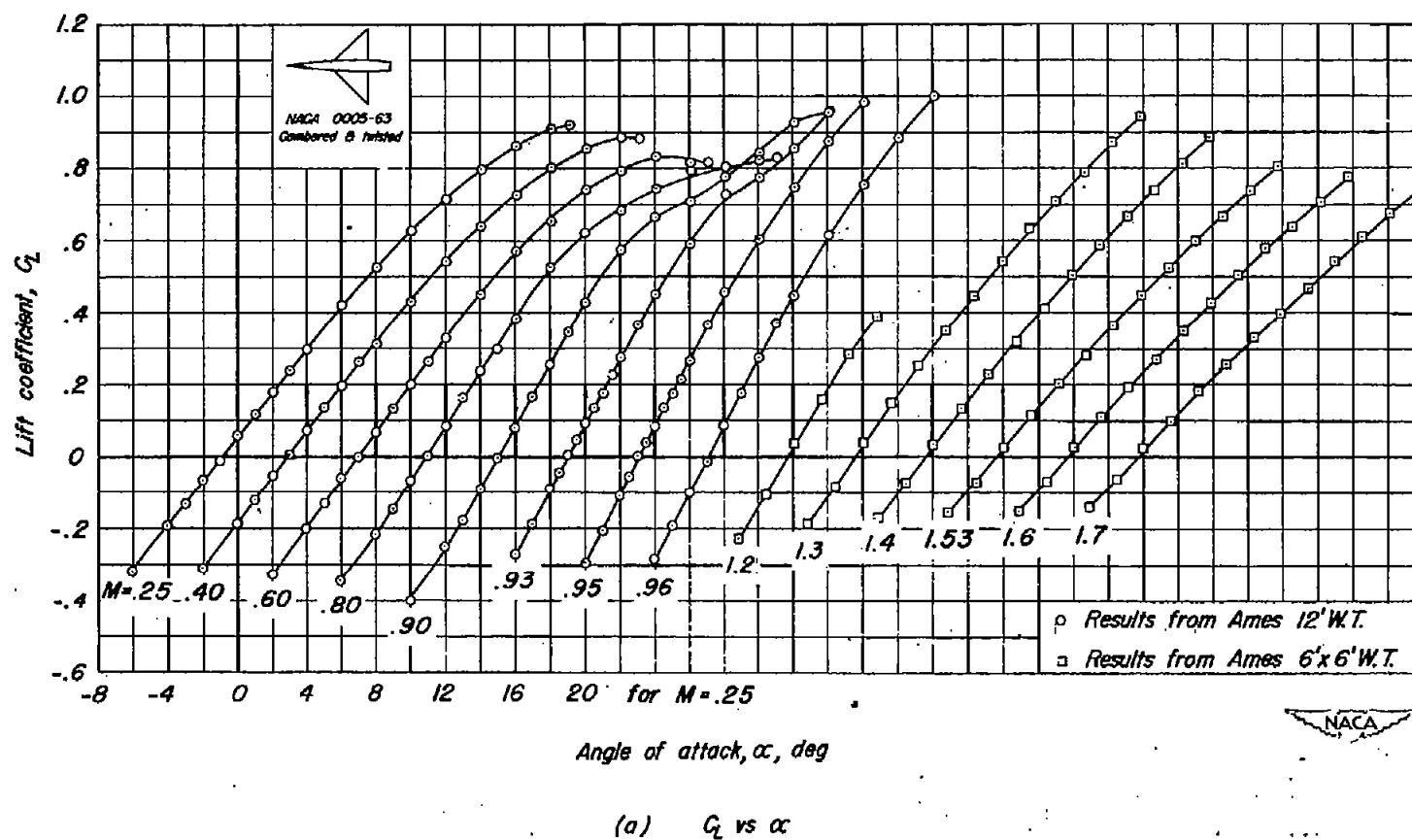
Figure 3.- The variation of the aerodynamic characteristics with lift coefficient at various Mach numbers.

Reynolds number, 1.5 million.
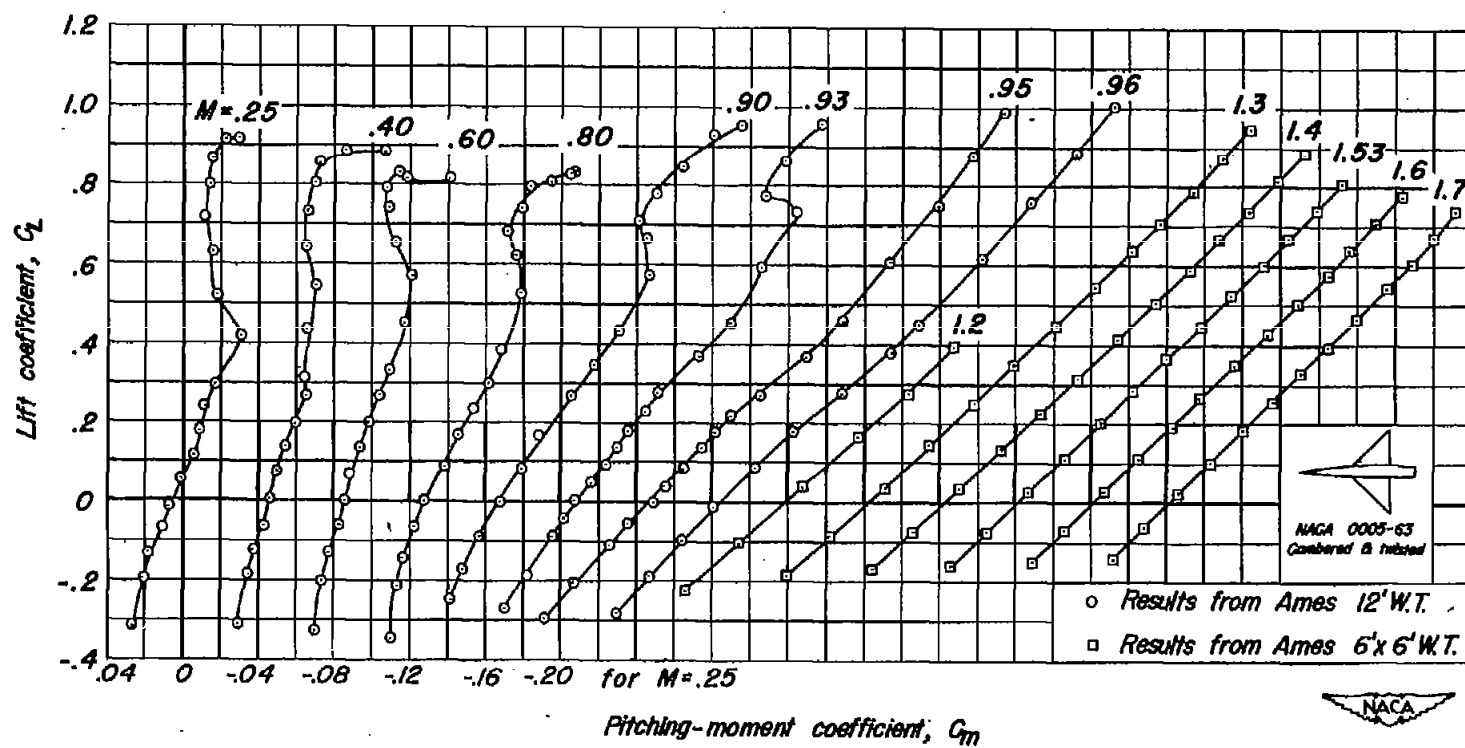
(b) C_L vs C_m

Figure 3.- Continued.
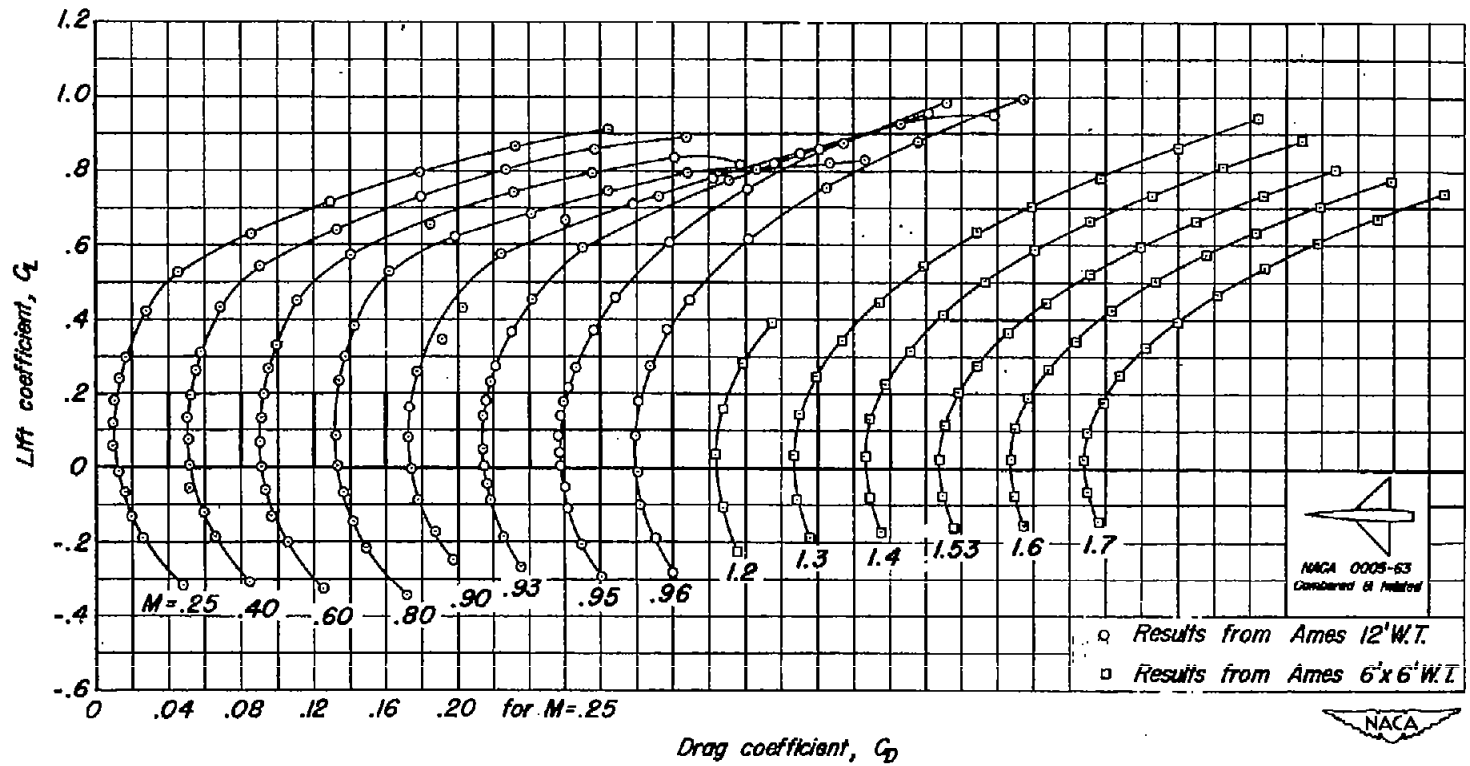
(c) C_L vs C_D

Figure 3.- Continued.
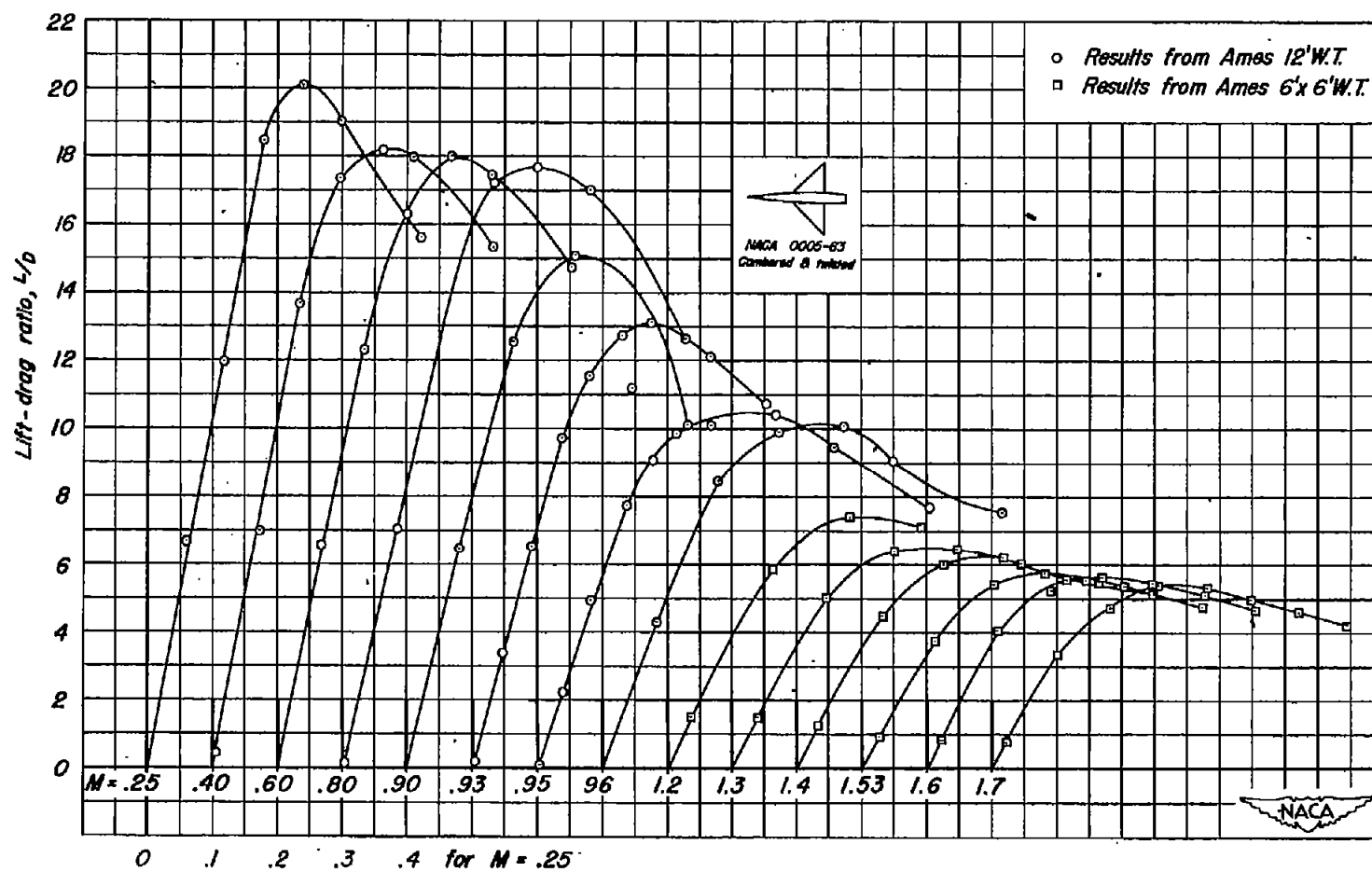
(d) L/D vs C_L

Figure 3.- Concluded.
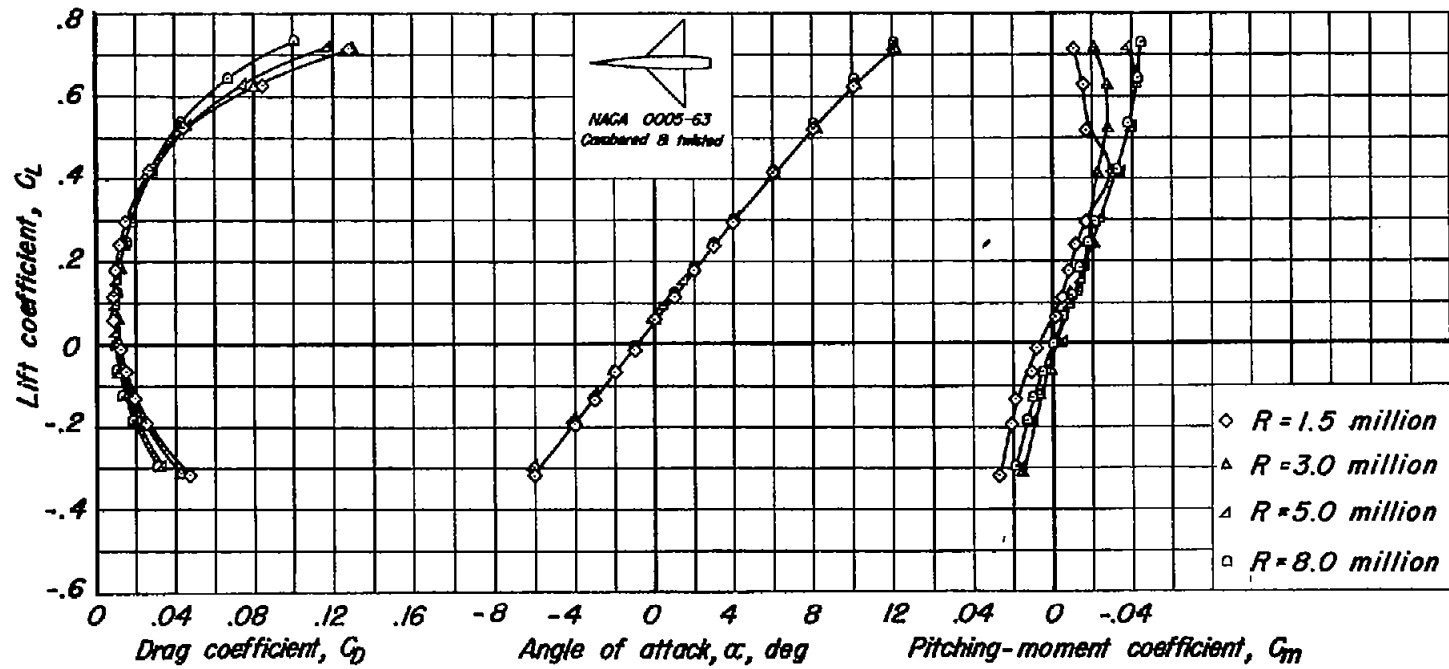
(a)   M=.25

Figure 4.- The variation of the aerodynamic characteristics with lift coefficient
at various Reynolds numbers.

NACA 0005-63
Cambered & twisted

◇ R = .75 million
△ R = 1.5 million
△ R = 3.0 million

(b) M = 1.2

Figure 4.- Continued.

NACA 0005-63
Cambered & twisted

Lift coefficient, C_L

Drag coefficient, C_D

Angle of attack, α, deg

Pitching-moment coefficient, C_m
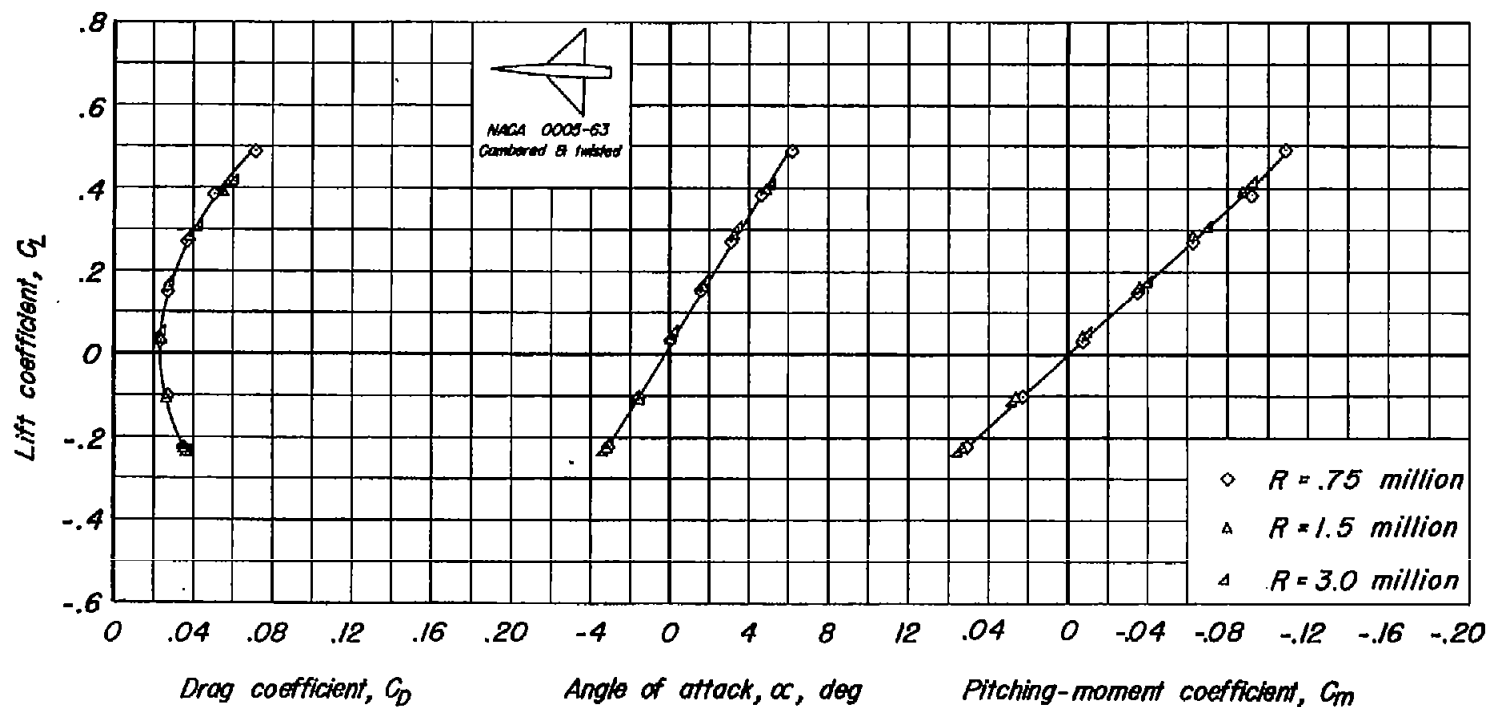
◇ R = .75 million
△ R = 1.5 million
⊿ R = 3.0 million
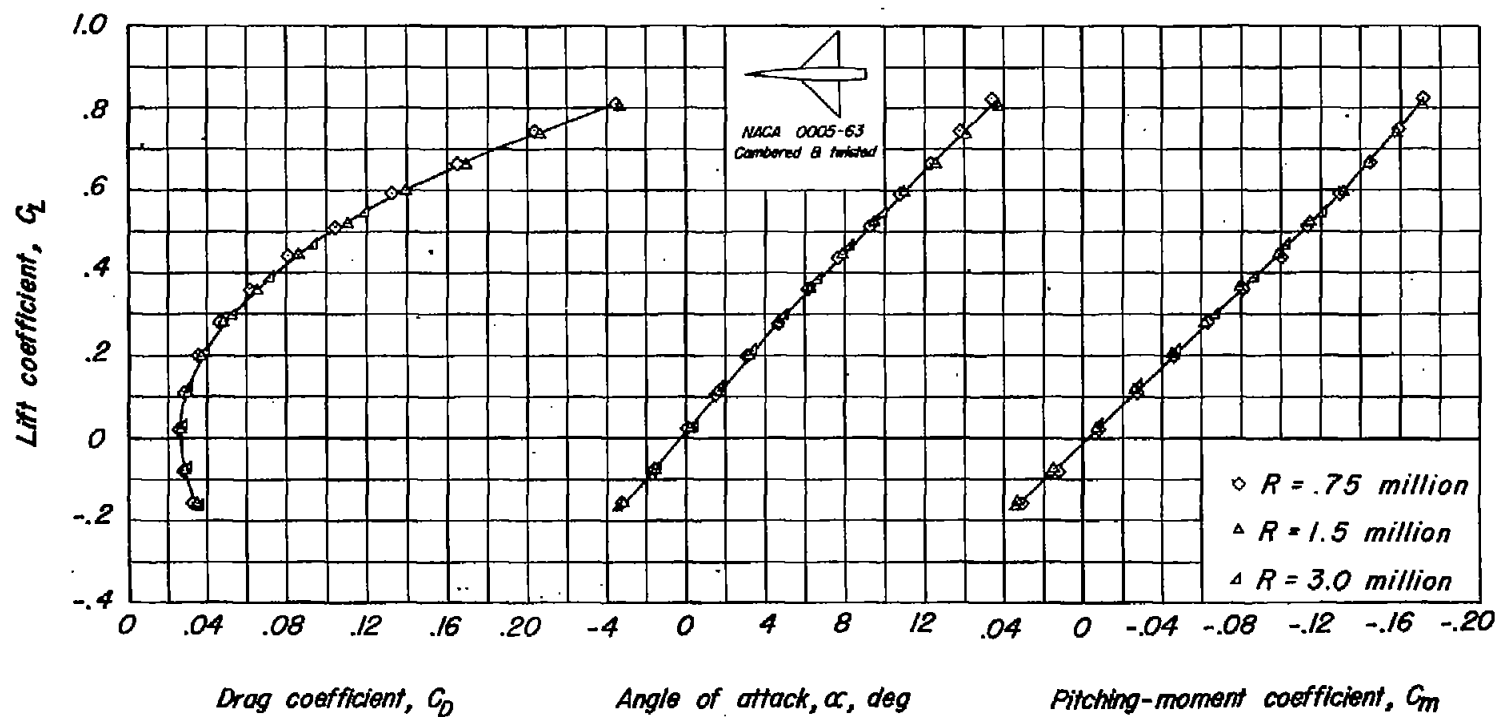
(c)   M=1.53

Figure 4.- Concluded.
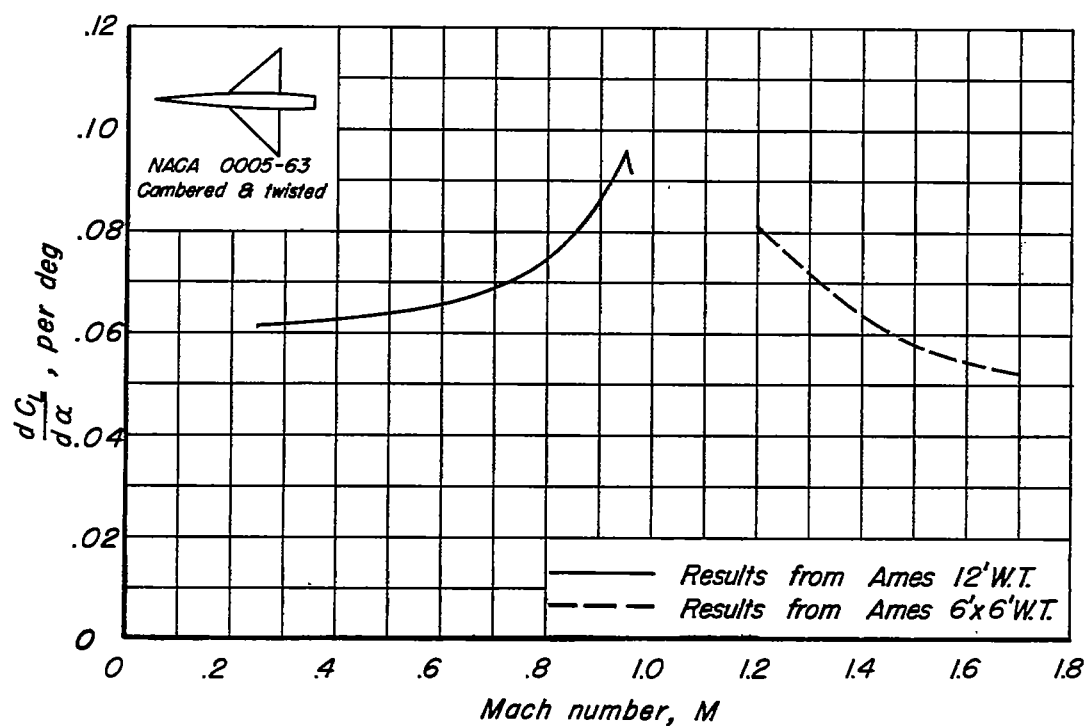
(a) $\dfrac{dC_L}{d\alpha}$ vs M
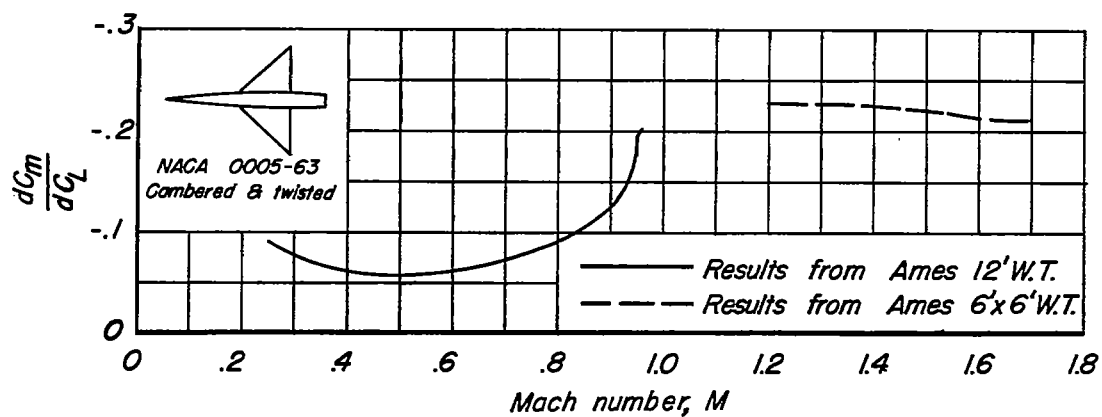
(b) $\dfrac{dC_m}{dC_L}$ vs M

Figure 5.- Summary of aerodynamic characteristics as a function of Mach number. Reynolds number, 1.5 million.
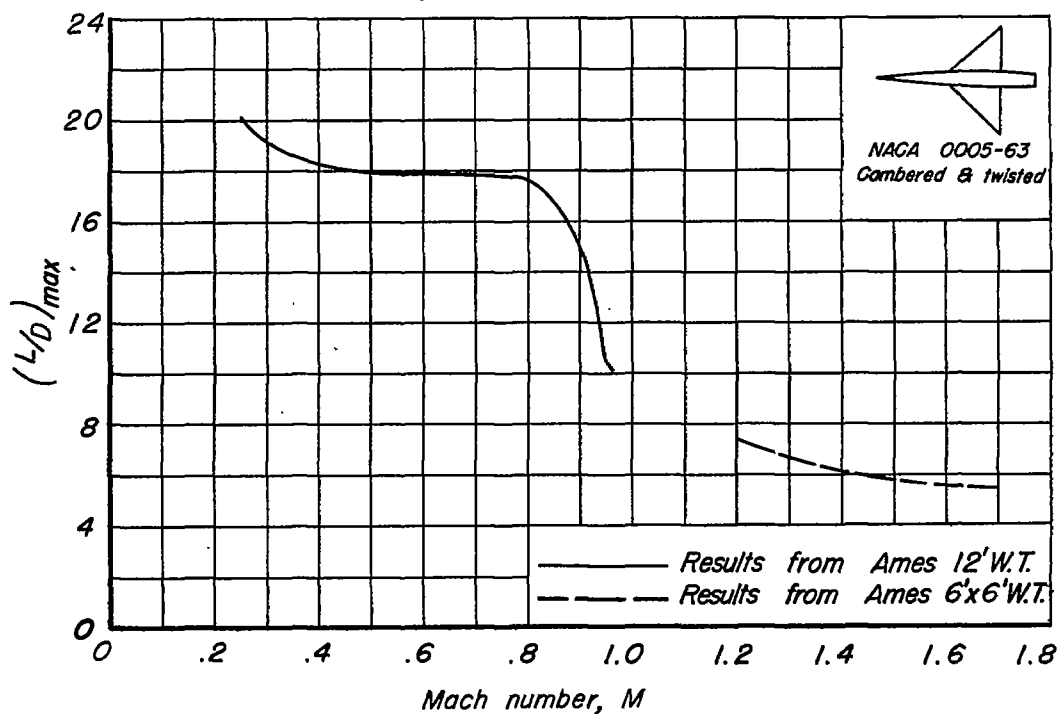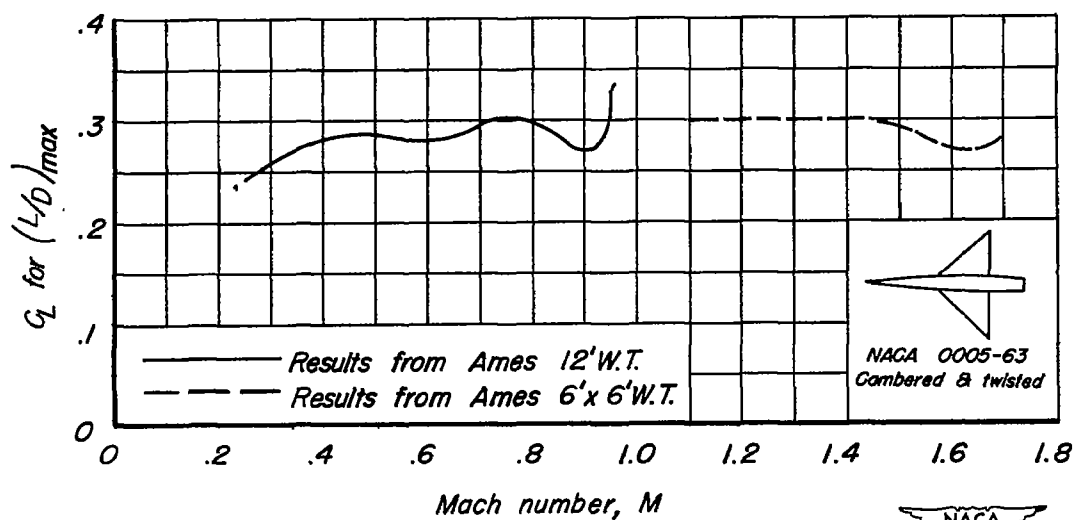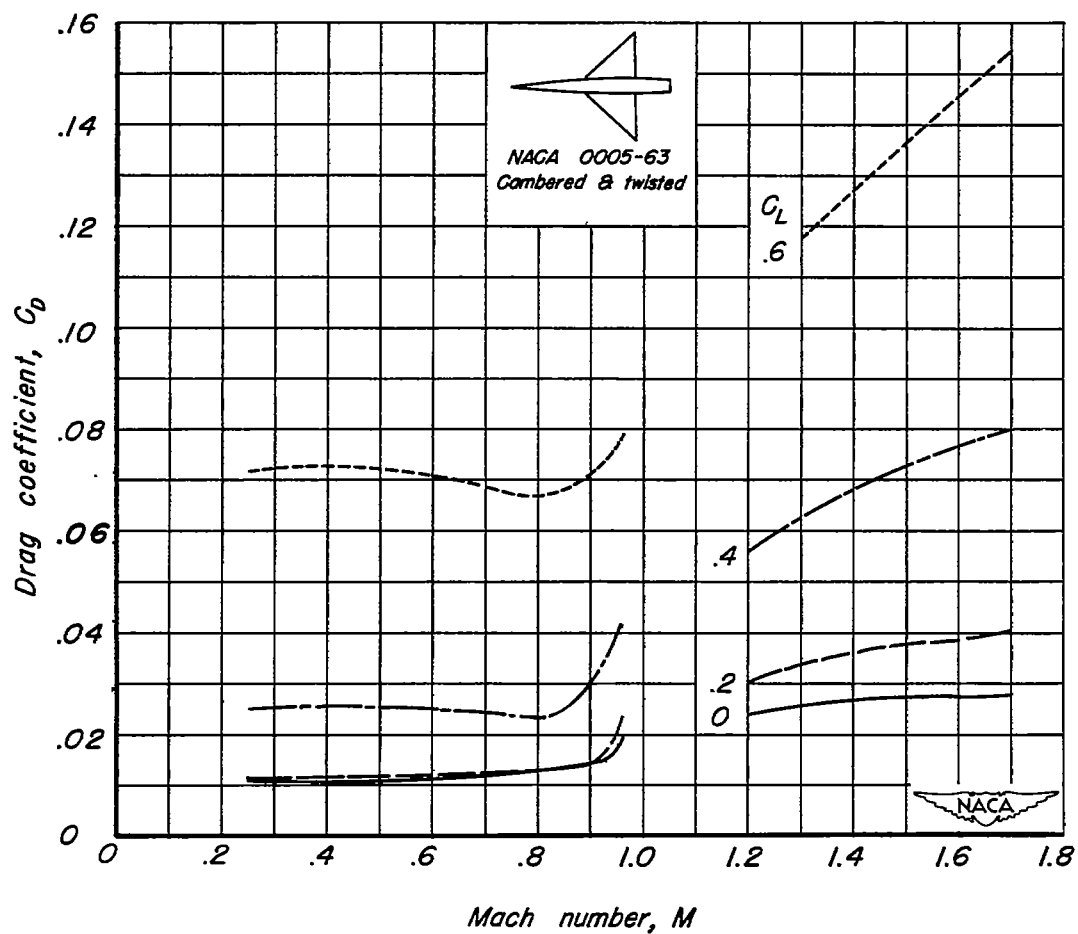
(c) $\left(L/D\right)_{max}$ vs M

(d) C_L for $\left(L/D\right)_{max}$ vs M.

Figure 5.- Continued.

(e) C_D vs M.

Figure 5.- Concluded.